Journal of Thermal Analysis and Calorimetry (2022) 147:1299–1306
https://doi.org/10.1007/s10973-020-10479-3

Thermal study and characterization of new cocrystals of ciprofloxacin with picolinic acid

Carolina Torquetti[1] · Patrícia Osório Ferreira[1] · Amanda Cosmo de Almeida[1] · Richard Perosa Fernandes[2] · Flávio Junior Caires[1,2]

Received: 2 May 2020 / Accepted: 9 December 2020 / Published online: 5 February 2021

Abstract

This article describes the mechanochemical synthesis (liquid-assisted grinding (LAG) and neat grinding (NG)), characterization and thermoanalytical study of new cocrystals of ciprofloxacin (CIP) with picolinic acid (PCA) in a 1:1 molar ratio. Characterization was performed through thermoanalytical techniques (differential scanning calorimetry (DSC), simultaneous thermogravimetry and differential scanning calorimetry (TG-DSC)), X-ray powder diffraction (XRPD) and infrared spectroscopy (IR). The thermoanalytical study, together with the XRPD and IR techniques, confirmed the formation of new cocrystal and helped to understand its formation. From the LAG method, using ethanol as a solvent, a cocrystal solvate was obtained. The NG method, together with thermal stress, favored obtaining the cocrystal through a coamorphous intermediate phase. Solubility study of all new materials showed an increase in CIP concentration for the cocrystals compared to pure drug.

Keywords Ciprofloxacin · Cocrystal · Cocrystal solvate · Coamorphous · Mechanochemistry · Thermal analysis

Introduction

The pharmaceutical market is one of the most important sectors in global economy and is supposed to reach the revenue of $1170 trillion in 2021, growing at 5.8% according to pharma market research report [1]. Among the challenges inside pharmaceutical field, solubility has been reported as a constant problem in the pipeline of drug development [2]. The bioavailability is direct correlated to the aqueous solubility of these drugs in the gastrointestinal tract. In this way, approaches that increase drug solubility have been a common topic in recent pharmaceutical research [3].

Cocrystallization has emerged as a promising method that modifies the physicochemical properties of drugs without affecting the specificity of pharmaceutical compounds [4, 5]. Cocrystal has been reported as an alternative to enhance solubility, dissolution rate, hygroscopicity, and physical and chemical stability of active pharmaceutical ingredients (API) [6–8]. Pharmaceutical cocrystals are generally crystalline materials composed of one API molecule and at least one other molecule called coformer [6]. Coformers need to be safe to human consumption and be part of "generally recognized as safe" (GRAS) substances regulated by Food and Drug Administration (FDA) [4].

Ciprofloxacin (CIP) is an antimicrobial agent (antibiotic) that acts against the proliferation of Gram-positive and Gram-negative microorganisms. The substance is part of the fluoroquinolones class and has low aqueous solubility. It is widely used in the treatment of respiratory and urinary infections, among other diseases [9].

Cocrystals of CIP were previous obtained with nicotinic acid, isonicotinic acid, pyrazinoic acid and p-aminobenzoic acid by the mechanochemical method in the stoichiometric ratio of 1:1, with and without the addition of ethanol [10, 11]. The cocrystallization approach results in an aqueous solubility increase, showing the possibility to enhance the properties of the drug by cocrystal formation.

The picolinic acid (PCA) coformer, also known as pyridine-2-carboxylic acid, is a pyridine derivative that has in its ring a carboxylic acid group in position 2, and it is capable of forming 5-membered intramolecular O–H···N rings through the o-carboxylic group. The compound is formed naturally from the degradation of tryptophan, and it is considered a

✉ Flávio Junior Caires
flavio.caires@unesp.br

[1] São Paulo State University (UNESP), School of Science, Chemistry Department, Bauru, SP, Brazil

[2] São Paulo State University (UNESP), Institute of Chemistry, Post-Graduate Program in Chemistry, Araraquara, SP, Brazil

cheap and safe drug, presenting several pharmacological applications such as antiviral, antimicrobial, HIV-1 inhibitor, among others [12].

Thus, this paper reports the mechanochemical synthesis, thermoanalytical study and characterization of new cocrystals between CIP and PCA (structural formula of the separated compounds presented in Fig. 1), as well as its evaluation by the solubility test.

Experimental

Material

CIP (purity ≥ 98%) and PCA (purity = 98%) were purchased from Sigma-Aldrich and used as received. Monopotassium phosphate (purity = 98%) and dipotassium phosphate (purity = 98%) from Anidrol and Synth, respectively.

Mechanochemical synthesis

The mechanochemical synthesis of CIP-PCA cocrystal in a 1:1 (*n*/*n*) stoichiometric ratio was performed in a Retsch MM 400 vibratory ball mill (Retsch, Germany) using stainless steel jars (10 mL volume) and a single ball of stainless steel (7 mm diameter) inside each jar.

To the mechanochemical synthesis were used the liquid-assisted grinding (LAG) and the neat grinding (NG) methods, with a total of 500 mg of sample, 30 Hz of frequency for 30 min. In the LAG method, ethanol was used, based on the principles of green chemistry, in the ratio of 0.25 μL mg^{-1} (volume of liquid added/total sample mass used in the grinding), as determined by Friscic and coauthors [13]. The neat grinding (NG) is a mechanochemical method that does not require liquid [14].

Characterization techniques

Simultaneous thermogravimetry and differential scanning calorimetry (TG-DSC) and differential scanning calorimetry (DSC) curves were obtained with two thermal analysis system, model TGA/DSC 1 and DSC 1 Star^e System, both from Mettler-Toledo (Zurich, Switzerland). The purge gas was a dynamic dry air atmosphere at a flow rate of 50 mL min^{-1}, heating rate of 10 °C min^{-1}, with samples masses of 5 mg for TG-DSC and 2.5 mg for DSC. Crucibles of α-alumina (150 μL) and aluminum (40 μL), the latter with perforated lid, were used for TG-DSC and DSC, respectively. DSC cell was calibrated for temperature and enthalpy by using indium metal (T_{melt} onset = 156.6 °C; ΔH_{fus} = 28.7 J g^{-1}) with 99.999% purity, according to manufacturer's instructions.

IR spectra were recorded using a Thermo Scientific Nicolet iS10 FTIR Spectrometer (Massachusetts, USA) equipped with a Thermo Scientific™ Smart iTX™ universal ATR sampling accessory with germanium crystal. Spectra were measured in the range from 4000 to 700 cm^{-1} with 32 accumulations and a resolution of 4 cm^{-1}.

Powder X-ray diffractograms (XRPD) were obtained using a Rigaku MiniFlex X-ray diffractometer (Tokyo, Japan), employing CuKα radiation (λ = 1.54056 Å), an operating voltage of 40 kV and current of 15 mA. The samples were placed on glass support and analyzed from 5° to 50° (2θ) at a scan speed of 4° min^{-1} (continuous scan mode).

Solubility determination

The shake-flask saturation method was applied in these solubility assays. Approximately 15 mg of each sample was placed in a test tube containing 5 mL of phosphate buffer solution (pH 6.8). The samples were held for 24 h in a shaker incubator from Marconi (Sao Paulo, Brazil), at 37 °C and 60 rpm. Then, the samples were filtered through PTFE membrane syringe filters with 0.2 μm pores and analyzed on a UV–Vis spectrophotometer. This test was performed in triplicate.

The quantification of the drug was performed in triplicate using an Agilent Technologies UV–Vis spectrophotometer, model Cary 845, in quartz cuvettes with 1.0 cm optical path at a fixed wavelength of 277 nm using a previously validated method [10]. The linear equation of the analytical curve is $y = 0.1282x + 0.0056$, with a correlation coefficient equal to 0.9999.

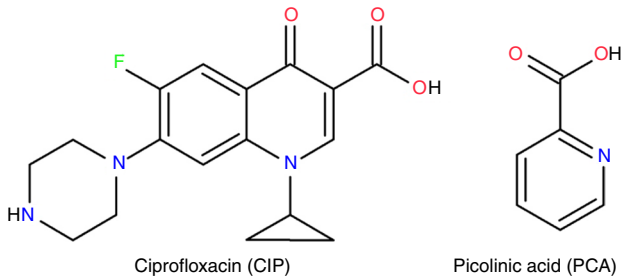

Fig. 1 Structural formula of compounds

Results and discussion

Thermal analysis

The TG-DSC and DSC curves of CIP, PCA and synthesized material are shown in Fig. 2a, b, respectively.

The TG-DSC and DSC curves of CIP show an endothermic peak at 268 °C (TG-DSC) and 270 °C (DSC, ΔH = 35.02 kJ mol^{-1}) related to the drug melting, with no

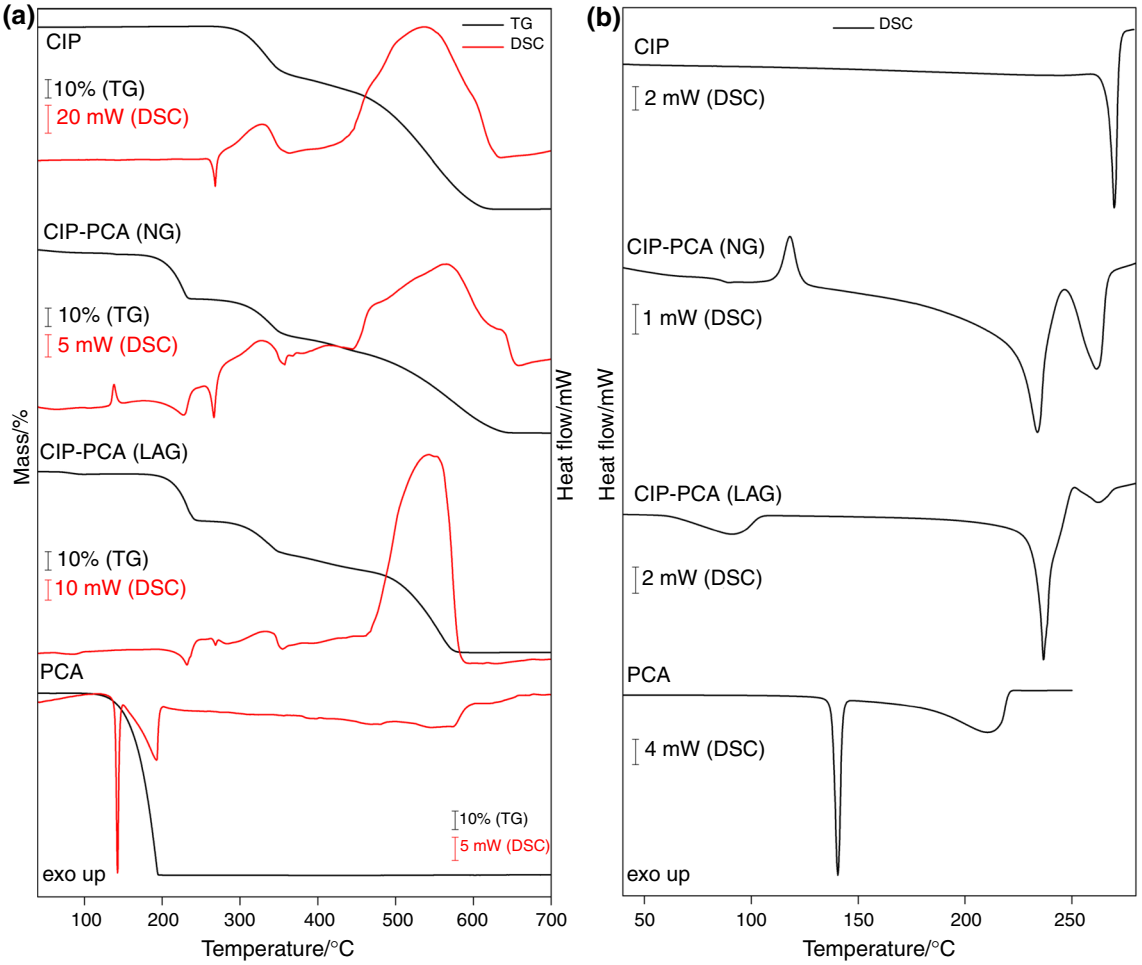

Fig. 2 **a** TG-DSC curves and **b** DSC curves of isolated precursors and CIP-PCA (1:1) systems obtained by NG and LAG synthesis method

mass loss in TG curve. These curves show that the drug is thermally stable up to 280 °C and undergoes thermal decomposition in three consecutive mass loss steps, corresponding to exothermic events in the DSC curves. All results in agreement with previous reports [10, 11].

The TG-DSC and DSC curves of PCA are in agreement with those reported by Nascimento and coauthors [15]. Mass loss begins by partial sublimation of the sample at 110 °C, the compound melts at 143 °C (TG-DSC) or 140 °C (DSC, $\Delta H = 26.08$ kJ mol^{-1}), and it undergoes thermal decomposition up to 195 °C, corresponding to the exothermic event at 193 °C (TG-DSC) and 211 °C (DSC).

The CIP-PCA systems exhibit a similar thermal stability of 180 °C for NG and LAG material according to TG curve, higher than PCA and lower than CIP. No thermal event associated with the melting of the system is observed. The system undergoes thermal decomposition in three steps of mass loss, corresponding to endothermic and exothermic events in the DSC curve. The first mass loss step occurs between 30–86 °C for CIP-PCA (NG) ($\Delta m_1 = 2.09\%$) and 30–110 °C for CIP-PCA (LAG) ($\Delta m_1 = 1.35\%$), relative to the small and broad endothermic peaks at 66 °C (CIP-PCA (NG)) and 86 °C (CIP-PCA (LAG)), attributed to water/solvent loss. The second mass loss occurs between 180 and 240 °C (CIP-PCA (NG) $\Delta m_2 = 27.06\%$; CIP-PCA (LAG) $\Delta m_2 = 26.65\%$), corresponding to the endothermic event at 228 °C (CIP-PCA (NG)) and 232 °C (CIP-PCA (LAG)) in the DSC curve, attributed to the beginning of the thermal decomposition of the CIP-PCA system with picolinic acid degradation ($\Delta m_{\text{theor.}} = 26.61\%$). Above 251 °C, the thermal behavior followed steps very similar to CIP, presenting the same steps of thermal decomposition and melting peak at 268 °C.

In relation to the differences between CIP-PCA (LAG) and CIP-PCA (NG) systems, the CIP-PCA (NG) system exhibits an exothermic event at 138 °C in DSC curve, with no mass loss in the TG curve, which may be attributed to a physical phenomenon that will be further discussed. This thermal event is not observed in the DSC curve of the CIP-PCA (LAG) system.

The DSC curve of CIP-PCA (LAG) shows three endothermic peaks at 91 °C, 237 °C and 263 °C, attributed to the desolvation, thermal decomposition and melting of CIP, respectively, while the DSC curve of CIP-PCA (NG) shows an exothermic peak at 116 °C and two endothermic peaks at 235 °C and 258 °C, attributed to a physical process, thermal decomposition and melting of CIP, respectively.

In addition, the baseline of the DSC curve of CIP-PCA (NG) system has a small deviation between 80 and 88 °C, characteristic of the glass transition ($T_g = 84$ °C) of amorphous materials [16], which will be discussed in the XRPD section.

The temperature range (θ), mass losses (Δm), peak temperatures (T_p) and enthalpies (ΔH) observed in the TG-DSC and DSC curves of the precursors and CIP-PCA systems are summarized in Table 1.

XRPD

The diffractograms of pure components and CIP-PCA systems obtained by the NG and LAG methods are shown in Fig. 3.

The CIP-PCA (NG) system exhibits a diffraction pattern that resemble the pharmacological component, with the major peaks of CIP at 25.32°, 20.6° and 14.28° are still present. In addition, a diffraction halo is also observed, which suggests that during the grinding process part of the material could have been amorphized, as already reported for other cocrystals obtained by the NG method [17, 18] and in agreement the glass transition observed in the DSC curve.

The exothermic event at 118 °C in DSC curve of CIP-PCA (NG) was investigated by XRPD, analyzing the heated material up to 100 °C and 130 °C (samples were cooled until ambient temperature before XRPD analysis). There is an increase in the diffraction halo intensity and some peaks attributed to the precursors disappear at 100 °C, probably due to the rapid cooling of the sample after heating it to temperatures above the glass transition temperature. Above the exothermic peak, the sample exhibits a new diffraction pattern, suggesting that the thermal event is related to cocrystallization process [16, 18]. These results suggest that the formation process of the new multicomponent crystalline phase occurs through an amorphous intermediate phase, as already reported for other systems [17, 18].

The XRPD diffractogram of CIP-PCA (LAG) system exhibits a distinct diffraction pattern when compared to precursor diffractograms, which confirms the formation of a new crystalline phase.

The DSC event observed at 91 °C in the DSC curve and previous discussed was investigated by XRPD (heating the material up to 115 °C and analyzing the cooled material). A new XRPD pattern is observed, indicating that the event is relative to desolvation and suggesting that solvent molecules are part of the crystal structure of the new multicomponent solid, probably a cocrystal solvate.

For the LAG synthesis method, it was not possible to detect the presence of the amorphous phase as intermediate,

Table 1 Thermoanalytical data obtained from the TG-DSC and DSC curves of the precursors and the CIP-PCA (1:1) systems

Compounds	TG-DSC					DSC				
		Thermal event[a]	1st step	2nd step	3rd step	A	B	C	D	E
CIP	θ/°C	–	280–360	360–700	–	–	–	–	–	–
	Δm/%	–	25.75	74.32	–	–	–	–	–	–
	T_p/°C	270↓	334↑	546↑	–	–	–	–	–	270↓
	ΔH/kJ mol^{-1}	–	–	–	–	–	–	–	–	5.02
PCA	θ/°C	–	115–200	–	–	–	–	–	–	–
	Δm/%	–	97.91	–	–	–	–	–	–	–
	T_p/°C	143↓	192↓	–	–	–	–	–	211↓	140↓
	ΔH/kJ mol^{-1}	–	–	–	–	–	–	–	55.12	26.08
CIP-PCA (NG)	θ/°C	–	30–86	180–240	251–360	–	–	–	–	–
	Δm/%	–	2.09	27.06	19.27	–	–	–	–	–
	T_p/°C	133↑	58↓	227↓	267↓	–	88*	118↑	234↓	262↓
	ΔH/kJ mol^{-1}	–	–	–	–	–	0.24	– 13.12	93.92	35.17
CIP-PCA (LAG)	θ/°C	–	30–110	180–240	257–375	–	–	–	–	–
	Δm/%	–	1.35	26.65	18.77	–	–	–	–	–
	T_p/°C	–	81↓	233↓	271↓	91↓	–	–	237↓	263↓
	ΔH/kJ mol^{-1}	–	–	–	–	35.25	–	–	161.64	11.66

θ: Temperature ranges; Δm: mass losses; T_p: peak temperatures; ΔH: enthalpies; ↑: exothermic peak; ↓: endothermic peak; [a]: physical process; *: T_g; A: desolvation; B: glass transition; C: cocrystallization; D: thermal decomposition; E: melting

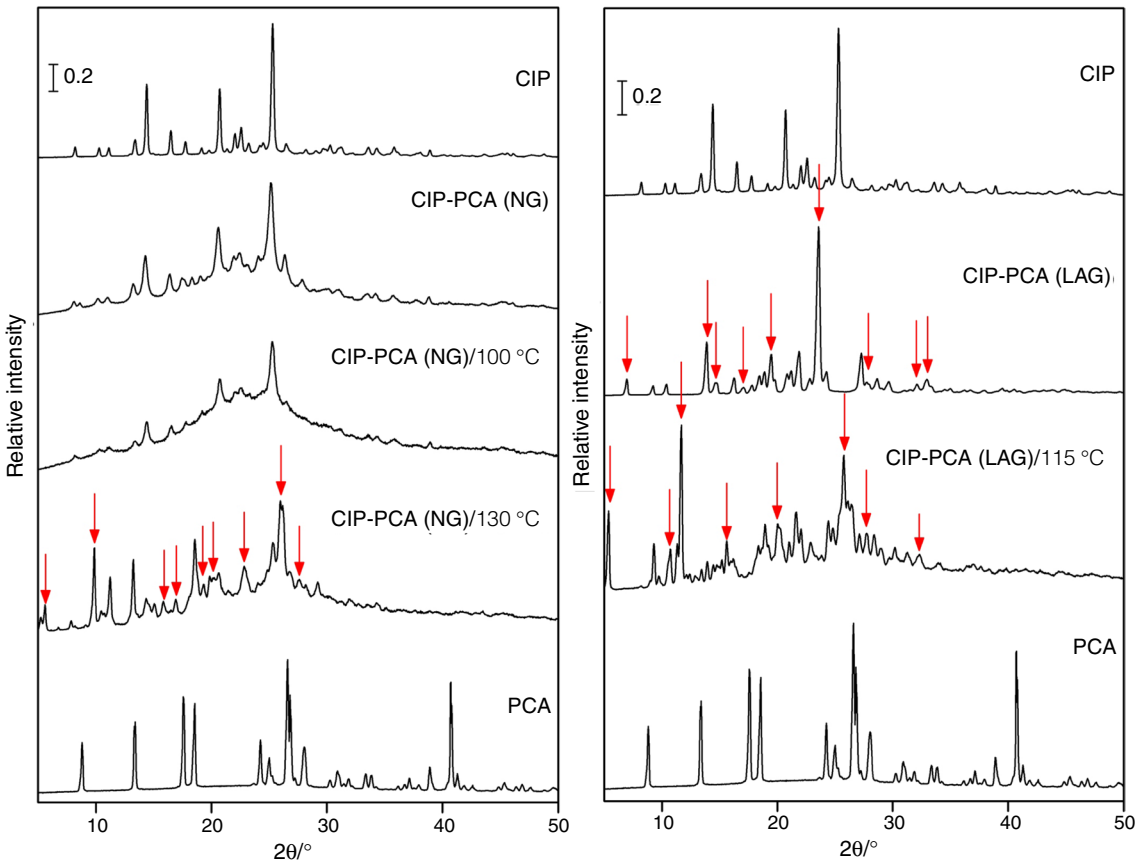

Fig. 3 XRPD diffraction patterns of isolated precursors and CIP-PCA (1:1) systems obtained by NG and LAG synthesis method

as in the case of the system obtained by the NG synthesis method, probably because the solvent acts as a catalyst for the cocrystallization process [17, 19].

In addition, it should be noted that the diffractogram of the CIP-PCA (NG)/130 °C system is different from that obtained for the CIP-PCA (LAG)/115 °C system, which shows that the conditions of formation of the crystalline phase lead to different polymorphic forms, as already reported [20].

IR spectroscopy

The IR spectra of precursors and CIP-PCA systems obtained by NG and LAG method are shown in Fig. 4.

The pharmaceutical compound CIP exhibits similar profile when compared to literature data [21], with strong bands observed at 1375 cm^{-1} (ν_{sym} COO^-), 1589 cm^{-1} (ν_{asym} COO^-), 1617 cm^{-1} (ν $C{=}O_{ketone}$) and small ones in the region of 2580–2680 cm^{-1} (ν NH_2^+ group). These bands show that CIP is in zwitterionic form [22].

IR spectrum of 2-picolinic acid exhibits bands at 1439 cm^{-1} (ν $(C{=}C)_{aromatic\ ring}$), 1650 cm^{-1} (ν $(C{=}N)_{aromatic\ ring}$) and 1712 cm^{-1} (ν $C{=}O_{COOH}$). In addition, the broad band between 2607 and 2152 cm^{-1} is attributed to the existence of $COOH{\cdots}N_{aromatic\ ring}$ intramolecular hydrogen bonds, which may disappear when new intermolecular interactions are formed [12].

For the IR spectra of the CIP-PCA systems, the bands attributed to the stretch vibrations of the carboxylate and NH_2^+ groups appear around the same wavelength as that observed for the isolated drug. However, there is a decrease in band intensity attributed to ν_{asym} COO^- of the carboxylate group, suggesting that this group may be participating in the multicomponent interactions. The band attributed to the ν $C{=}O_{ketone}$ is shifted to longer wavelengths (1628 cm^{-1}). Other bands (unassigned) attributed to vibrational modes of the drug molecule undergo shifts to lower wavelengths. The band attributed to the carbonyl group (ν $C{=}O_{COOH}$) is much more intense and shifts to higher wavelengths (1728 cm^{-1}). In addition, the band attributed to intense intermolecular interactions ($COOH{\cdots}N_{aromatic\ ring}$) is no longer observed.

In addition, the spectrum of the CIP-PCA (NG) system is very similar to that of the CIP-PCA (NG)/130 °C system, which suggests that supramolecular synthons had already been established in the CIP-PCA (NG) system.

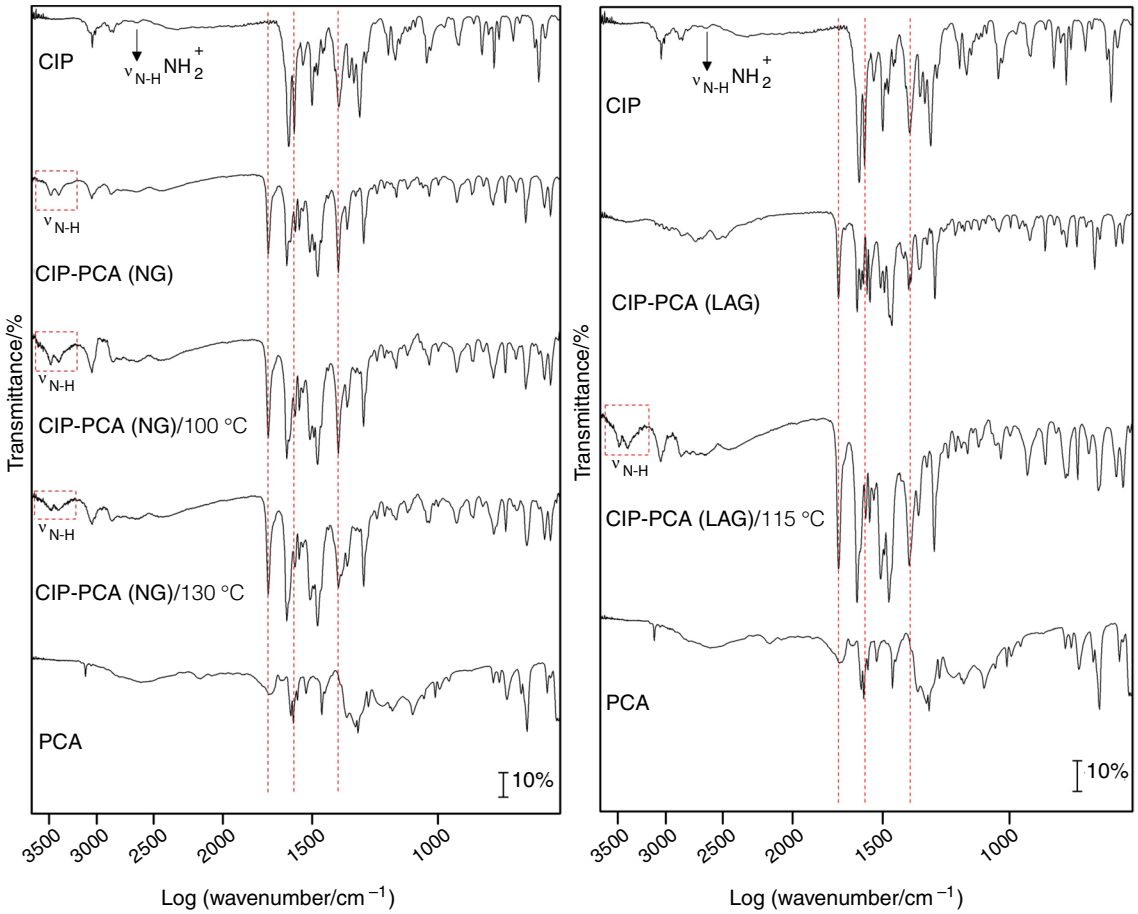

Fig. 4 IR spectra of isolated precursors and CIP-PCA (1:1) systems obtained by NG and LAG synthesis method

This confirms the formation of a coamorphous phase before cocrystal formation, according to the XRPD results.

Lastly, these results suggest that the carboxylate group of CIP and the carbonyl group of PCA are the main groups involved in the formation of supramolecular synthons. In addition, the bands attributed to the carboxylate group vibrations of the PCA coformer are not observed, which excludes the possibility of salt formation and confirms that the multicomponent crystalline phase is a cocrystal (CIP-PCA (LAG) and coamorphous (CIP-PCA (NG)) [23]. These results are similar to those observed for ciprofloxacin cocrystals with nicotinic and isonicotinic acid isomers [10].

Solubility study

All materials synthesized (NG and LAG) and studied through thermal analysis, IR spectroscopy and XRPD technique were evaluated in solubility studies, and results are shown in Fig. 5.

The solubility study shows the minor result for CIP (139.64 ± 0.01 μg mL^{-1}) and maximum result for CIP-PCA (NG) (178.08 ± 0.02 μg mL^{-1}). Cocrystals showed an increase in concentration of 1.12x (CIP-PCA (LAG)), 1.18x (CIP-PCA (NG)/130 °C), 1.21x (CIP-PCA (LAG)/115 °C) and 1.27x (CIP-PCA (NG)) compared to pure drug. The

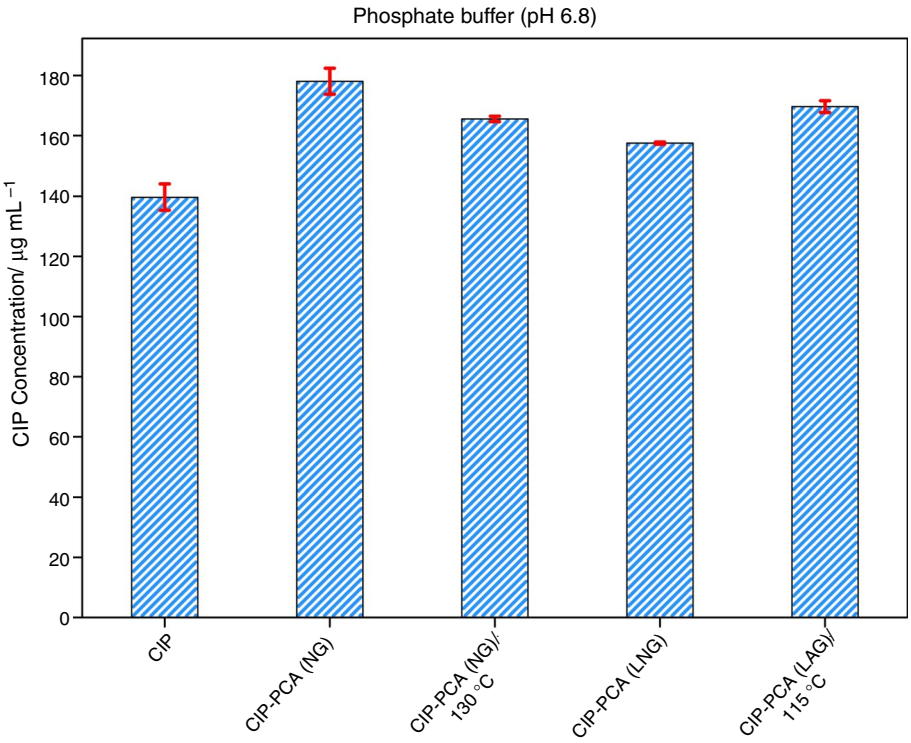

Fig. 5 Solubility test of CIP and CIP-PCA (1:1) systems obtained by NG and LAG synthesis method. (pH 6.8 and 37 °C, $n=3$)

solvate (CIP-PCA (LAG)) and anhydrous (CIP-PCA (LAG)/115 °C) results are in agreement with behavior of anhydrates/solvate compounds, where the anhydrates forms usually possess higher solubility when compared to solvate forms for pharmaceutical compounds [24]. Besides, the partially coamorphous sample (CIP-PCA (NG)) resulted in the maximum solubility observed when compared to the other samples, which can be explained for the tendency of coamorphous solids to have higher solubility [25, 26].

Conclusions

The mechanochemical synthesis with and without solvent was effective as a screening technique to obtain cocrystals between CIP and PCA; the method could be presented as an alternative to solution-based approaches or others methods due to the low proportion of the materials used, resulting in low cost in terms of energy and resources.

Thermal analysis was essential to identify and understand the formation of new CIP-PCA cocrystals. TG-DSC and DSC with the complementary techniques, XRPD and IR, confirmed the formation of least two polymorphs of the CIP-PCA cocrystals (CIP-PCA (NG)/130 °C and CIP-PCA (LAG)/115 °C), a cocrystal solvate (CIP-PCA (LAG) and a partially coamorphous solid (CIP-PCA (NG)). The IR spectra suggest that the interaction between molecules occurs through the carboxylate group of CIP and the carbonyl group of PCA.

The solubility study of the new materials showed that cocrystallization can improve aqueous solubility of CIP, with an increase in CIP concentration in 6.8 phosphate buffer of 27% compared to pure drug.

Acknowledgements The authors thank CPID/CDMF, FAPESP (Grant Nos. 2013/09022-7, 2015/19863-4, 2017/14936-9, 2018/12463-9 and 2018/24378-6), CNPq (Grant Nos. 141829/2017-6, 421469/2016-1, 133104/2019-2) and CAPES (Grant No. 001) foundations (Brazil) for financial support.

References

1. Company TBR. Pharmaceutical Drugs Global Market Report 2018 Including: Musculoskeletal Disorder Drugs; Cardiovascular Drugs; Oncology Drugs; Anti-infective Drugs; Metabolic Disorder Drugs; Central Nervous System Drugs; Genito-urinary Drugs; Gastrointestinal Drugs; He. 2018.
2. Savla R, Browne J, Plassat V, Wasan KM, Wasan EK. Review and analysis of FDA approved drugs using lipid-based formulations. Drug Dev Ind Pharm. 2017. https://doi.org/10.1080/03639045.2017.1342654.
3. Mantri RV, Sanghvi R, Zhu HJ. Solubility of pharmaceutical solids. Dev Solid Oral Dos Forms Pharm Theory Pract Second Ed. 2017. https://doi.org/10.1016/B978-0-12-802447-8.00001-7.
4. Karagianni A, Malamatari M, Kachrimanis K. Pharmaceutical cocrystals: new solid phase modification approaches for

the formulation of APIs. Pharmaceutics. 2018. https://doi.org/10.3390/pharmaceutics10010018.
5. Fernandes RP, do Nascimento ALCS, Carvalho ACS, Teixeira JA, Ionashiro M, Caires FJ. Mechanochemical synthesis, characterization, and thermal behavior of meloxicam cocrystals with salicylic acid, fumaric acid, and malic acid. J Therm Anal Calorim. 2019; https://doi.org/10.1007/s10973-019-08118-7.
6. Schultheiss N, Newman A. Pharmaceutical cocrystals and their physicochemical properties. Cryst Growth Des. 2009. https://doi.org/10.1021/cg900129f.
7. Bruni G, Monteforte F, Maggi L, et al. Probenecid and benzamide: cocrystal prepared by a green method and its physico-chemical and pharmaceutical characterization. J Therm Anal Calorim. 2019. https://doi.org/10.1007/s10973-019-09197-2.
8. Fuliaş A, Vlase G, Vlase T, Şuta LM, Şoica C, Ledeţi I. Screening and characterization of cocrystal formation between carbamazepine and succinic acid. J Therm Anal Calorim. 2015. https://doi.org/10.1007/s10973-015-4473-8.
9. Martin Santos A, Wong A, Araújo Almeida A, Fatibello-Filho O. Simultaneous determination of paracetamol and ciprofloxacin in biological fluid samples using a glassy carbon electrode modified with graphene oxide and nickel oxide nanoparticles. Talanta. 2017. https://doi.org/10.1016/j.talanta.2017.06.040.
10. de Almeida AC, Torquetti C, Ferreira PO, Fernandes RP, dos Santos EC, Kogawa AC, Caires FJ. Cocrystals of ciprofloxacin with nicotinic and isonicotinic acids: mechanochemical synthesis, characterization, thermal and solubility study. Thermochim Acta. 2020. https://doi.org/10.1016/j.tca.2019.178346.
11. de Almeida AC, Ferreira PO, Torquetti C, Ekawa B, Carvalho ACS, dos Santos EC, Caires FJ. Mechanochemical synthesis, characterization and thermal study of new cocrystals of ciprofloxacin with pyrazinoic acid and *p*-aminobenzoic acid. J Therm Anal Calorim. 2019. https://doi.org/10.1007/s10973-019-08958-3.
12. Tella AC, Oladipo AC, Adeyemi OG, Oluwafemi OS, Oguntoye SO, Alimi LO, Ajayi JT, Degni SK. Solid state synthesis, spectroscopic and X-ray studies of metal complexes of 2-picolinic acid and vapochromic behavior of $[Co(Pic)2(H_2O)2]\cdot 2H_2O$. Solid State Sci. 2017. https://doi.org/10.1016/j.solidstatesciences.2017.03.017.
13. Friščić T, Childs SL, Rizvi SAA, Jones W. The role of solvent in mechanochemical and sonochemical cocrystal formation: a solubility-based approach for predicting cocrystallisation outcome. CrystEngComm. 2009. https://doi.org/10.1039/B815174A.
14. Douroumis D, Ross SA, Nokhodchi A. Advanced methodologies for cocrystal synthesis. Adv Drug Deliv Rev. 2017. https://doi.org/10.1016/j.addr.2017.07.008.
15. Do Nascimento ALCS, Teixeira JA, Nunes WDG, Campos FX, Treu-Filho O, Caires FJ, Ionashiro M. Thermal behavior, spectroscopic study and evolved gas analysis (EGA) during pyrolysis of picolinic acid, sodium picolinate and its light trivalent lanthanide complexes in solid state. J Anal Appl Pyrol. 2016. https://doi.org/10.1016/j.jaap.2016.01.010.
16. D'Angelo A, Edgar B, Hurt AP, Antonijević MD. Physico-chemical characterisation of three-component co-amorphous systems generated by a melt-quench method. J Therm Anal Calorim. 2018. https://doi.org/10.1007/s10973-018-7291-y.
17. Jayasankar A, Somwangthanaroj A, Shao ZJ, Rodríguez-Hornedo N. Cocrystal formation during cogrinding and storage is mediated by amorphous phase. Pharm Res. 2006. https://doi.org/10.1007/s11095-006-9110-6.
18. Seefeldt K, Miller J, Alvarez-Núñez F, Rodríguez-Hornedo N. Crystallization pathways and kinetics of carbamazepine-nicotinamide cocrystals from the amorphous state by in situ thermomicroscopy, spectroscopy and calorimetry studies. J Pharm Sci. 2012. https://doi.org/10.1002/jps.
19. Ross SA, Lamprou DA, Douroumis D. Engineering and manufacturing of pharmaceutical co-crystals: a review of solvent-free manufacturing technologies. Chem Commun. 2016. https://doi.org/10.1039/C6CC01289B.
20. Fischer F, Heidrich A, Greiser S, Benemann S, Rademann K, Emmerling F. Polymorphism of mechanochemically synthesized cocrystals: a case study. Cryst Growth Des. 2016. https://doi.org/10.1021/acs.cgd.5b01776.
21. Sahoo S, Chakraborti CK, Mishra SC, Nanda UN, Naik S. FTIR and XRD investigations of some fluoroquinolones. Int J Pharm Pharm Sci. 2011;.
22. Polishchuk AV, Karaseva ET, Emelina TB, Cramariuc O, Karasev VE. Polymorphism and intramolecular proton transfer in fluoroquinolone compounds. J Fluoresc. 2011. https://doi.org/10.1007/s10895-011-0912-5.
23. Cerreia Vioglio P, Chierotti MR, Gobetto R. Pharmaceutical aspects of salt and cocrystal forms of APIs and characterization challenges. Adv Drug Deliv Rev. 2017. https://doi.org/10.1016/j.addr.2017.07.001.
24. Huang LF, Tong WQ. Impact of solid state properties on developability assessment of drug candidates. Adv Drug Deliv Rev. 2004. https://doi.org/10.1016/j.addr.2003.10.007.
25. Dengale SJ, Grohganz H, Rades T, Löbmann K. Recent advances in co-amorphous drug formulations. Adv Drug Deliv Rev. 2016. https://doi.org/10.1016/j.addr.2015.12.009.
26. Shi Q, Moinuddin SM, Cai T. Advances in coamorphous drug delivery systems. Acta Pharm Sin B. 2019. https://doi.org/10.1016/j.apsb.2018.08.002.